

# Interaction between $\text{NO}_x$ and the Surface of Supported Heteropoly Compounds: In Situ IR Spectroscopic Data

V. A. Matyshak<sup>a</sup>, N. V. Konokhov<sup>a</sup>, V. F. Tret'yakov<sup>b</sup>, Yu. P. Tyulenin<sup>a</sup>,  
O. N. Sil'chenkova<sup>a</sup>, V. N. Korchak<sup>a</sup>, and Rui Wong<sup>c</sup>

<sup>a</sup> Semenov Institute of Chemical Physics, Russian Academy of Sciences, Moscow, 119991 Russia

<sup>b</sup> Topchiev Institute of Petrochemical Synthesis, Russian Academy of Sciences, 119991 Russia

<sup>c</sup> Shandong University, Jinan City, Shandong Province, China

e-mail: matyshak@chph.ras.ru

Received April 27, 2010

**Abstract**—The mechanism of activation of nitrogen oxides on unsupported heteropoly compounds and the composition, location, stability, and interconversion mechanisms of adsorption complexes on supported heteropoly compounds have been investigated by *in situ* IR spectroscopy under thermal desorption conditions. Supporting a small amount of a heteropoly compounds (1% or below) increases  $\text{NO}_x$  adsorption relative to the adsorption observed for the pure support. This effect is most pronounced for  $\text{CeO}_2$  and least pronounced for  $\text{ZrO}_2$ . The increase in  $\text{NO}_x$  adsorption is due to NO oxidation to  $\text{NO}_2$  on the supported heteropoly compound. The main adsorption species are nitrite and nitrate complexes, which are located on the support. As the temperature is raised, the nitrite complexes turn into the nitrate complexes. The presence of variable-valence ions in the Keggin anion reduces the nitrate complex–surface binding strength. The ions that are not components of the Keggin anion increase the binding strength. The changes in the nitrate complex–support surface binding strength are due to the support modification taking place via the destruction of part of the supported heteropoly compound.

**DOI:** 10.1134/S002315841103013X

One of the central present-day environmental problems is that of reducing the  $\text{NO}_x$  emissions from industrial facilities. This problem extends to gas turbines, heat power plants, and automotive internal combustion engines consuming diesel fuel. A promising way of solving this problem is catalytic reduction of nitrogen oxides under oxidative conditions. Two variants of this process have been considered in the literature.

The first variant needs effective catalysts for  $\text{NO}_x$  reduction to  $\text{N}_2$  with hydrocarbons in the presence of oxygen. The existing approaches to creating exhaust gas treatment catalysts are based on the known data concerning the mechanism of the selective reduction of nitrogen oxides in the presence of hydrocarbons [1–6].

Note that, although there have been numerous studies on various types of catalytic systems and reductants, the problem is still unsolved. This is largely due to the high oxygen concentration in diesel exhaust, which makes  $\text{NO}_x$  reduction to nitrogen much more difficult to carry out.

A possible way out is suggested by catalytic converters in which  $\text{NO}_x$  is trapped and, as soon as the trap is filled, fuel is injected for a short time and desorbed  $\text{NO}_x$  is reduced over a three-way catalyst—second variant of the process [7–9].

Catalytic converters generally contain  $\text{NO}_x$ -adsorbing components (alkali metal and alkaline-earth metal oxides), noble metals (usually Pt or Rh), and a support with a large specific surface area (usually  $\gamma\text{-Al}_2\text{O}_3$ ) [10]. In recent years, there have been publications on catalysts supported on mixed oxides consisting of  $\text{TiO}_2$ ,  $\text{ZrO}_2$ ,  $\text{Al}_2\text{O}_3$ , and  $\text{CeO}_2$  [11, 12] or on hydrotalcite [13]. There has been a comparative study of the effect of the support ( $\text{MgO}$ ,  $\text{Al}_2\text{O}_3$ ,  $\text{ZrO}_2$ ,  $\text{SiO}_2$ ) on the formation of adsorbed nitrates and on the rate of their reduction with hydrogen [12].

Numerous studies have been aimed at elucidating the detailed mechanism of  $\text{NO}_x$  accumulation and reduction [14–24]. The effects of  $\text{CO}_2$  and  $\text{SO}_2$  on  $\text{NO}_x$  adsorption and reductions were reported [25, 26]. Note that the greater part of these data refers to  $\text{Pt/Ba-Al}_2\text{O}_3$  catalysts. It is conventionally believed that the first stage of  $\text{NO}_x$  removal is NO oxidation to  $\text{NO}_2$  on Pt sites. The nitrogen oxide  $\text{NO}_2$  is desorbed as nitrites and nitrates on alkali or alkaline-earth metal oxides and then undergoes spillover to the support.

A literature survey demonstrated that search for new, efficient  $\text{NO}_x$  neutralization catalysts, as well as the investigation of the mechanism of this process, should be continued. Here, we report the mechanism of  $\text{NO}_x$  adsorption and activation on supported het-

eropoly compounds (HPCs), a new class of catalysts. A specific feature of HPCs is that they have an ultramicroporous structure with a mean pore size of 1–2 nm (depending on the heteropolyanion composition and cation type), which forms upon the removal of the water of crystallization from the initial heteropoly acid (HPA). By replacing metal atoms in heteropolyanions, one can obtain mixed HPCs containing different metal atoms. It is thus possible to vary the oxidation potential and acidity of HPCs in rather wide ranges. When supported on a solid, these structures can activate nitrogen oxide adsorption at low temperatures and favor their reduction by hydrocarbons at elevated temperatures.

The HPCs were supported on  $\theta\text{-Al}_2\text{O}_3$ ,  $\text{CeO}_2$ , or  $\text{ZrO}_2$ . These materials were chosen for the reason that  $\gamma$ -alumina doped with transition metal ions is unstable under hydrothermal treatment conditions and recrystallizes and transition metal cations migrate into the lattice [27]. The high-temperature alumina phase  $\theta\text{-Al}_2\text{O}_3$  suffers from this drawback to a much lesser extent. Cerium and zirconium dioxides are widely used as supports and structural and electronic promoters for enhancing the activity, selectivity, and thermal stability of catalysts. Cerium-containing materials have found widest use in redox processes owing to the capability of the fluorite structure to withstand high oxygen deficiency levels without changing its structural type [28, 29].

## EXPERIMENTAL

### Catalyst Preparation

Heteropoly compounds based on phosphomolybodic acid were obtained by solid-phase synthesis [30].

Supported catalysts were prepared by impregnating a support with an HPA or HPC solution (1, 5, 10, or 70% of the support weight) followed by drying at 120°C for 3 h and by stepwise calcination at 150, 180, 200, 220, and 250°C for 30–40 min at each temperature point. The products were thoroughly ground and were calcined again at 350°C for 1.5–2 h.

$\theta\text{-Al}_2\text{O}_3$  was obtained by calcination of commercial  $\gamma$ -alumina with a specific surface area of 217 m<sup>2</sup>/g in air at 300°C for 1 h and then at 800, 900, and 1100°C for 3 h at each temperature point. The specific surface area of the resulting  $\theta\text{-Al}_2\text{O}_3$  was 116 m<sup>2</sup>/g.

Cerium dioxide ( $S_{sp} = 79$  m<sup>2</sup>/g) was obtained by heating  $\text{Ce}(\text{NO}_3)_3 \cdot 6\text{H}_2\text{O}$  in air at a rate of 7 K/min to 500°C and by holding it at this temperature for 2 h.

Zirconium dioxide was obtained by calcination of zirconium nitrate in air at 500°C for 3 h. According to X-ray diffraction data, the resulting  $\text{ZrO}_2$  consisted of approximately equal amounts of monoclinic and tetragonal phases. The specific surface area of the oxide was 98 m<sup>2</sup>/g. The specific surface area of any support

loaded with 1%  $\text{KCu}_{0.25}\text{PMo}_{10}\text{VWO}_x$  was practically equal to that of the initial support.

### In Situ IR Spectroscopy

IR transmission spectra were obtained on a Spectrum RX I FT-IR System spectrometer (PerkinElmer) at 4 cm<sup>-1</sup> resolution with a one-scan time of 4.2 s. Use of quartz reactor cells with spectroscopic ZnS windows made it possible to record IR spectra in situ at elevated temperatures of up to 500°C [31].

The samples to be characterized by IR transmission spectroscopy were pressed into pellets at  $P = 5000$  kg/cm<sup>2</sup>. The thickness of a catalyst pellet was equivalent to 20–70 mg/cm<sup>2</sup>. The structure and properties of the surface complexes resulting from  $\text{NO}_x$  entrapment were studied by temperature-programmed desorption (TPD). Before being tested, the sample, placed in the reactor cell, was subjected to standard heat treatment in flowing  $\text{N}_2$  at 350°C for 30 min. After the sample cooled to room temperature,  $\text{NO}_x$  was adsorbed onto it from a 1000 ppm  $\text{NO} + \text{N}_2$  mixture (nitrogen contained approximately 1000 ppm  $\text{O}_2$  as an impurity). Thereafter, the cell was purged with a inert gas for removing weakly bound species and the sample was heated to 350°C at a constant rate in flowing  $\text{N}_2$ . IR spectra were recorded at each stage of this procedure. During  $\text{NO}_x$  TPD, IR spectra were recorded continuously. The time required for recording one spectrum was 4 min (60 scans). The concentration of surface complexes was estimated either in units of absorbance ( $A$ ) or from the integral intensity ( $A^*$ , cm<sup>-1</sup>) of absorption bands. All spectroscopic data presented in this work are converted to a pellet thickness of 20 mg/cm<sup>2</sup>.

The reaction temperature was controlled with a MINITERM-300.31 programmable temperature regulator. The deviation of the temperature from the preset value was <5°C. The composition of the gas phase before and after the reactor was determined using a Beckman-951A chemiluminescent  $\text{NO}/\text{NO}_x$  analyzer.

## RESULTS

### $\text{NO}_x$ Adsorption on Unsupported HPCs

Experiments were performed on  $\text{H}_3\text{PMo}_{12}\text{O}_{40}$  and on the following salts of this acid:  $\text{K}_{0.5}\text{PMo}_{11}\text{Sb}_{0.5}\text{W}_{0.5}\text{O}_x$ ,  $\text{K}_{0.5}\text{Nb}_{0.025}\text{PMo}_{11}\text{Sb}_{0.5}\text{W}_{0.5}\text{O}_x$ ,  $\text{K}_{0.5}\text{Nb}_1\text{PMo}_{11}\text{Sb}_{0.5}\text{W}_{0.5}\text{O}_x$ ,  $\text{KCu}_{0.25}\text{PMo}_{10}\text{SbWO}_x$ , and  $\text{KCu}_{0.25}\text{PMo}_{10}\text{VWO}_x$ .

Figure 1 presents the IR spectra recorded after  $\text{NO}_x$  adsorption on some of these compounds. It is evident that the unsupported HPCs almost do not adsorb  $\text{NO}_x$ . At the same time, the spectra show an absorption doublet around 1618 cm<sup>-1</sup>. This absorption characterizes the rotational-vibrational band contour of the  $\text{NO}_2$  molecule. Therefore, the unsupported HPCs are capable of oxidizing NO to  $\text{NO}_2$  at room temperature.

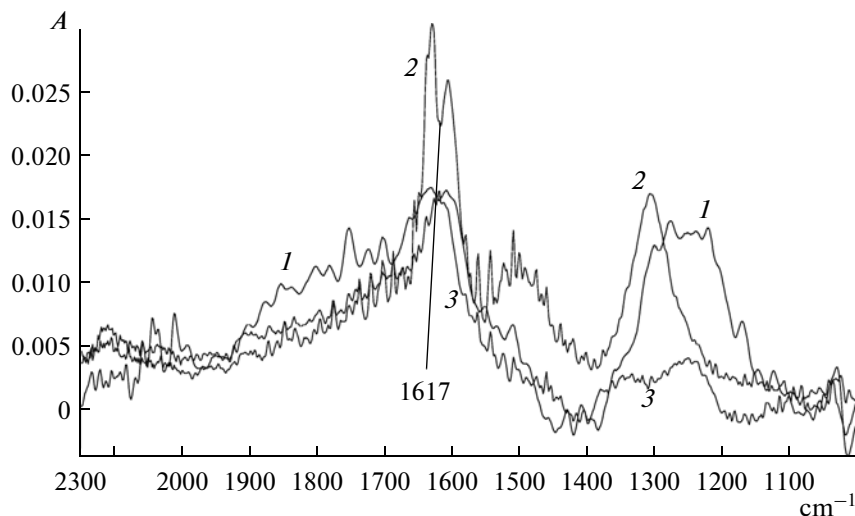


**Fig. 1.** IR spectra recorded after NO<sub>x</sub> adsorption at room temperature on the heteropoly compounds (1) K<sub>0.5</sub>Cu<sub>0.25</sub>PMo<sub>10</sub>SbWO<sub>x</sub>, (2) K<sub>0.5</sub>PMo<sub>11</sub>Sb<sub>0.5</sub>W<sub>0.5</sub>O<sub>x</sub>, and (3) K<sub>0.5</sub>PMo<sub>11</sub>Sb<sub>0.5</sub>W<sub>0.5</sub>Nb<sub>0.025</sub>O<sub>x</sub>.

#### NO<sub>x</sub> Adsorption on Supports

Figure 2 shows the spectra recorded after NO<sub>x</sub> adsorption on θ-Al<sub>2</sub>O<sub>3</sub>, CeO<sub>2</sub>, and ZrO<sub>2</sub> at room temperature (Fig. 2a) and after heating the samples to 280°C in flowing nitrogen (Fig. 2b).

Hereafter, the spectra are presented as the difference between the spectrum recorded after NO<sub>x</sub> adsorption and the spectrum taken of the initial solid at the same temperature.

The spectra of all of the supports after NO<sub>x</sub> adsorption at room temperature generally show absorption bands from two nitrite complexes and three nitrate complexes [11, 32] in different ratios. The positions and assignment of the observed absorption bands are presented in Table 1.

After NO<sub>x</sub> adsorption at room temperature, the largest amount of nitrite complexes (smallest amount of nitrate complexes) is observed for θ-Al<sub>2</sub>O<sub>3</sub> and the smallest amount of nitrite complexes (largest amount of nitrate complexes) is observed for ZrO<sub>2</sub>. This is likely due to the fact that the oxides differ in the properties of their surface oxygen.

As the temperature is raised, the absorption bands of the nitrite complexes weaken and those of the nitrate complexes strengthen. Because the temperature was increased in the absence of NO<sub>x</sub> in the gas phase, this trend of the band intensities indicates the conversion of the nitrite complexes into the nitrate complexes.

The bands of the nitrate complexes are fairly close together (Fig. 2), so it is difficult to determine the amount of each particular complex species. For this reason, the surface concentration of nitrate complexes was estimated in terms of the total area ( $A$ ,  $\text{cm}^{-1}$ ) of

the absorption bands of the nitrate complexes in the region of the high-frequency component of the  $v_3$  vibration (1500–1700  $\text{cm}^{-1}$ ).

Note the difference between the spectra of the supports after NO<sub>x</sub> adsorption. In the case of CeO<sub>2</sub> [33–37], NO<sub>x</sub> adsorption at room temperature yields surface complexes with *cis*- and *trans*-N<sub>2</sub>O<sub>2</sub><sup>2-</sup> and NO<sup>-</sup> structures. These complexes show themselves as absorption between 1100 and 1300  $\text{cm}^{-1}$ . The corresponding absorption bands complicate the spectrum of the nitrite and nitrate complexes on the CeO<sub>2</sub> surface (Fig. 2a). Note that, as the temperature is raised, the *cis*- and *trans*-N<sub>2</sub>O<sub>2</sub> and NO<sup>-</sup> structures in the presence of oxygen turn rapidly into nitrite and then nitrate complexes.

Among the supports examined, cerium dioxide possesses the best optical properties. Because of this, the absorption band at 798  $\text{cm}^{-1}$  arising from NO<sub>x</sub> adsorption can be observed only for this support (this spectral region is not shown in Fig. 2). Since the intensity of this band changes with temperature in the same way as the intensity of the absorption bands of the nitrate complexes, Philipp et al. [34] assigned this band to one of the vibrations in NO<sub>3</sub><sub>ads</sub>.

The adsorption of NO<sub>x</sub> on ZrO<sub>2</sub> yields considerable amounts of nitrate complexes even at room temperature. Furthermore, the amount of nitrate complexes on ZrO<sub>2</sub> is much larger than on the other supports (Fig. 2b), even though the supports have similar specific surface areas.

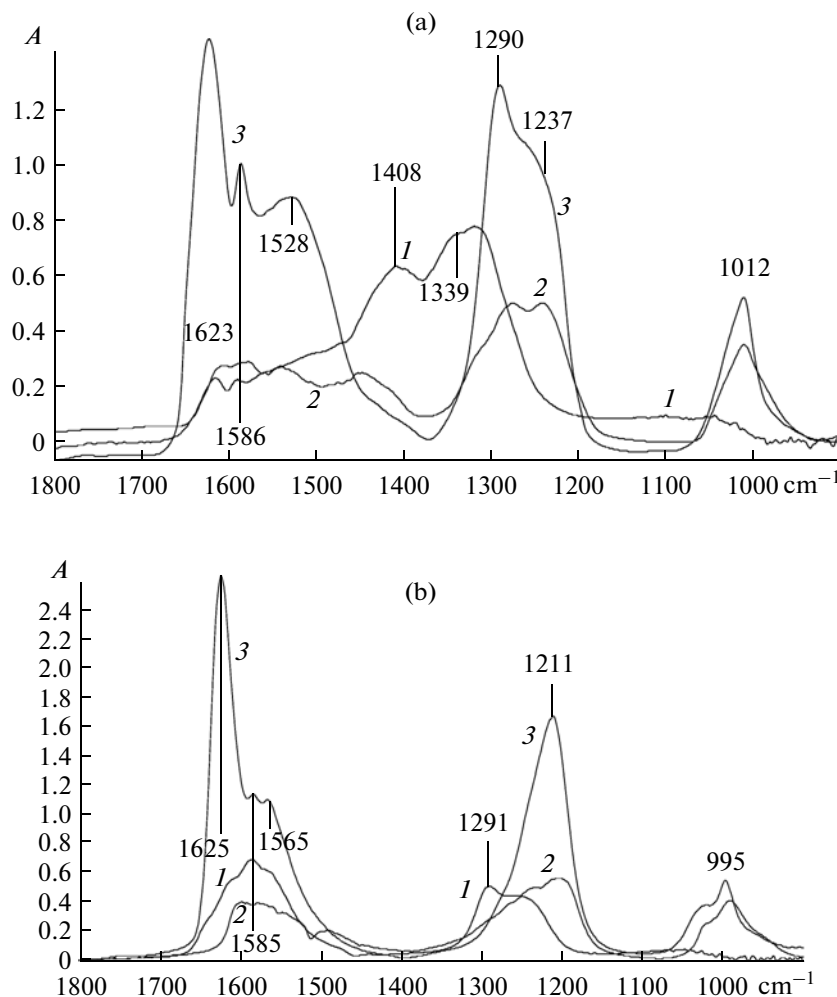


**Fig. 2.** IR spectra recorded (a) after  $\text{NO}_x$  adsorption on supports at room temperature and (b) after subsequent heating to 280°C in flowing nitrogen: (1)  $\theta\text{-Al}_2\text{O}_3$ , (2)  $\text{CeO}_2$ , and (3)  $\text{ZrO}_2$ .

#### Effect of the Supported HPC Concentration on $\text{NO}_x$ Adsorption

Figures 3 and 4 show the IR spectra recorded for the 1, 5, 10, and 70%  $\text{H}_3\text{PMo}_{12}\text{O}_{40}/\theta\text{-Al}_2\text{O}_3$  samples at different temperatures. Note that the spectrum of the surface complexes on the HPC-loaded samples is practically identical to the spectrum of the complexes

on the pure support. Therefore, the surface complexes of the HPC-loaded samples are located on the support, not on the supported HPC.

Supporting an HPC at a low concentration (1%) causes a marked increase in the amount of  $\text{NO}_x$  adsorbed as nitrite and nitrate complexes (Fig. 3, 1200–1700 cm<sup>-1</sup>). The same effect is observed for the

**Table 1.** Spectral characteristics of nitrite and nitrate complexes on different supports [11, 32] at room temperature

Complex	$\theta\text{-Al}_2\text{O}_3$	$\text{CeO}_2$	$\text{ZrO}_2$
Nitrite, bidentate	1317, 1410 cm <sup>-1</sup>	1275, 1320 cm <sup>-1</sup>	1290 cm <sup>-1</sup>
Nitrite, linear	1500 cm <sup>-1</sup>	1450 cm <sup>-1</sup>	1530 cm <sup>-1</sup>
Nitrate, bridging ( $\nu_3$ )	1617 cm <sup>-1</sup>	1600 cm <sup>-1</sup>	1625 cm <sup>-1</sup>
Nitrate, bidentate	1590 cm <sup>-1</sup>	1580 cm <sup>-1</sup>	1585 cm <sup>-1</sup>
Nitrate, linear	1566 cm <sup>-1</sup>	1545 cm <sup>-1</sup>	1555 cm <sup>-1</sup>

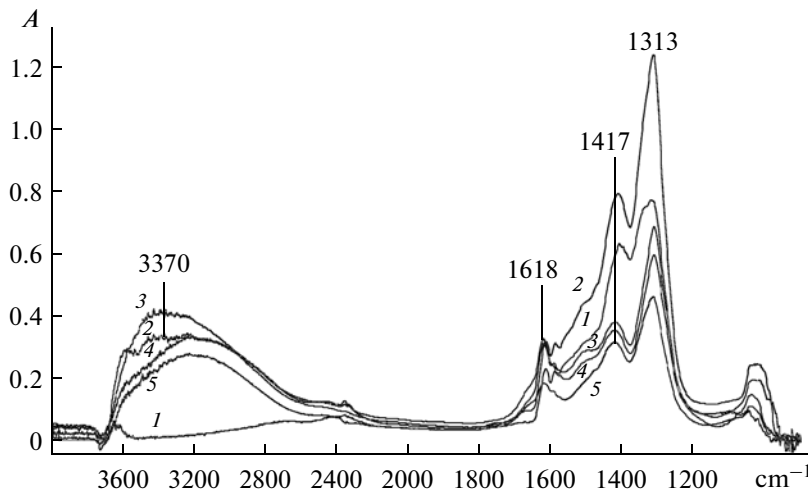


**Fig. 3.** IR spectra recorded after  $\text{NO}_x$  adsorption on  $\text{H}_3\text{PMo}_{12}\text{O}_{40}/\theta\text{-Al}_2\text{O}_3$  samples at room temperature: (1)  $\theta\text{-Al}_2\text{O}_3$ , (2) 1%  $\text{H}_3\text{PMo}_{12}\text{O}_{40}/\theta\text{-Al}_2\text{O}_3$ , (3) 5%  $\text{H}_3\text{PMo}_{12}\text{O}_{40}/\theta\text{-Al}_2\text{O}_3$ , (4) 10%  $\text{H}_3\text{PMo}_{12}\text{O}_{40}/\theta\text{-Al}_2\text{O}_3$ , and (5) 70%  $\text{H}_3\text{PMo}_{12}\text{O}_{40}/\theta\text{-Al}_2\text{O}_3$ .

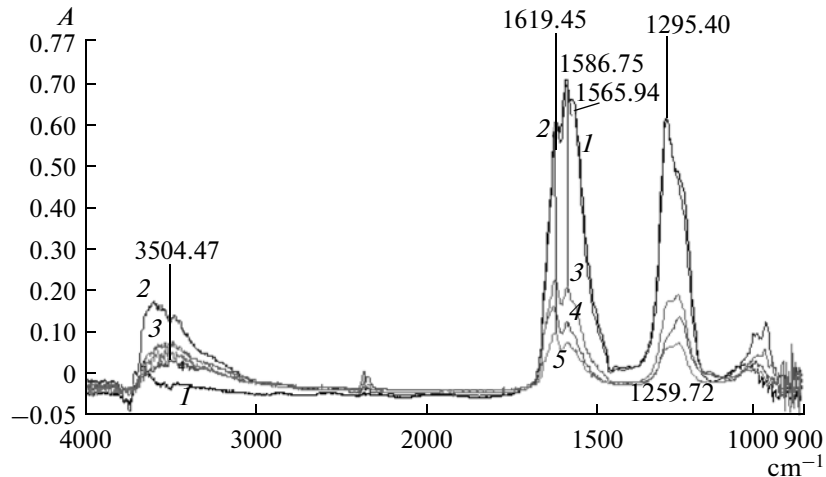


**Fig. 4.** IR spectra recorded after  $\text{NO}_x$  adsorption on  $\text{H}_3\text{PMo}_{12}\text{O}_{40}/\theta\text{-Al}_2\text{O}_3$  samples at room temperature and subsequent heating to 150°C in flowing nitrogen: (1)  $\theta\text{-Al}_2\text{O}_3$ , (2) 1%  $\text{H}_3\text{PMo}_{12}\text{O}_{40}/\theta\text{-Al}_2\text{O}_3$ , (3) 5%  $\text{H}_3\text{PMo}_{12}\text{O}_{40}/\theta\text{-Al}_2\text{O}_3$ , (4) 10%  $\text{H}_3\text{PMo}_{12}\text{O}_{40}/\theta\text{-Al}_2\text{O}_3$ , and (5) 70%  $\text{H}_3\text{PMo}_{12}\text{O}_{40}/\theta\text{-Al}_2\text{O}_3$ .

$\text{CeO}_2$ -based samples. Figure 5 presents the temperature dependences of the amount of the nitrate complexes resulting from  $\text{NO}_x$  adsorption for  $\text{CeO}_2$ , 1%  $\text{H}_n\text{PMo}_{11}\text{V}_1\text{O}_{40}/\text{CeO}_2$ , and 1%  $\text{H}_n\text{PMo}_9\text{V}_3\text{O}_{40}/\text{CeO}_2$ .

Supporting an HPC on  $\text{CeO}_2$  results in a greater increase in the amount of nitrate complexes than supporting the same HPC on  $\theta\text{-Al}_2\text{O}_3$ . The best results were obtained with the HPC whose Keggin anion contains three vanadium atoms.

The increase in the amount of nitrate complexes is likely due to weakly bound surface species because, at elevated temperatures (Fig. 4), the amounts of nitrate complexes on  $\theta\text{-Al}_2\text{O}_3$  and 1% HPC/ $\theta\text{-Al}_2\text{O}_3$  are nearly equal.

An opposite effect was observed for the  $\text{ZrO}_2$ -based samples. Supporting any amount of HPC onto  $\text{ZrO}_2$  (as distinct from  $\theta\text{-Al}_2\text{O}_3$  and  $\text{CeO}_2$ ) leads to a decrease in the amount of nitrate complexes relative to that adsorbed on the pure support (Table 2). The complex-surface binding strength remains practically unchanged.

As the supported HPC concentration is increased, the amount of adsorbed  $\text{NO}_x$  decreases (Figs. 3, 4). This is likely due to the blocking of part of the support surface. This effect is most pronounced for  $\text{ZrO}_2$  (Table 2) and least pronounced for  $\text{CeO}_2$  (Table 3). In the latter case, even supporting 5% HPC increases the amount of nitrate complexes. By contrast, supporting

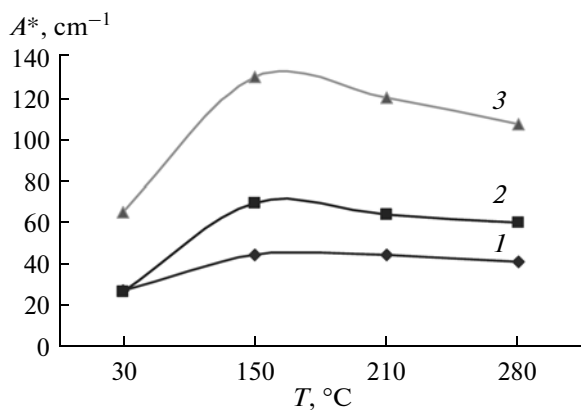


**Fig. 5.** Temperature dependence of the amount of nitrate complexes for (1) CeO<sub>2</sub>, (2) 1% H<sub>n</sub>PMo<sub>11</sub>V<sub>1</sub>O<sub>40</sub>/CeO<sub>2</sub>, and (3) 1% H<sub>n</sub>PMo<sub>9</sub>V<sub>3</sub>O<sub>40</sub>/CeO<sub>2</sub>.

>1% of any HPC onto θ-Al<sub>2</sub>O<sub>3</sub> leads to a decrease in NO<sub>x</sub> adsorption.

Note that NO<sub>x</sub> adsorption on the HPC-loaded samples (as distinct from NO<sub>x</sub> adsorption on the support (Fig. 2)) causes a considerable buildup of hydrogen-bonded hydroxyl groups on the surface (Figs. 3, 4) in the case of θ-Al<sub>2</sub>O<sub>3</sub> and ZrO<sub>2</sub>. For the CeO<sub>2</sub>-based samples, NO<sub>x</sub> adsorption does not change the spectrum of hydroxyl groups.

#### *Effect of the Composition of the Supported HPC on NO<sub>x</sub> Adsorption*

Investigation of NO<sub>x</sub> adsorption on materials containing different HPAs (1%) demonstrated that it is possible to vary the nitrate complex–surface binding strength. The data presented in Table 4 show how the amount of nitrate complexes on the surface of θ-Al<sub>2</sub>O<sub>3</sub>-supported HPAs with different vanadium contents varies with temperature up to 280°C.

At T > 150°C, the amount of nitrate complexes on the V-containing HPCs is smaller than on the support (Table 4). This means that the nitrate complex–sur-

**Table 2.** Temperature-dependent amounts of nitrate complexes (A\*) for the ZrO<sub>2</sub>-based catalysts

Catalyst/T, °C	30°C	150°C	210°C	280°C
ZrO <sub>2</sub>	32	164	164	159
1% KCu <sub>0.5</sub> PMo <sub>10</sub> VWO <sub>x</sub> /ZrO <sub>2</sub>	37	110	110	105
1% Ba <sub>0.5</sub> KPMo <sub>12</sub> O <sub>40</sub> /ZrO <sub>2</sub>	17	106	107	103
5% KCu <sub>0.5</sub> PMo <sub>10</sub> VWO <sub>x</sub> /ZrO <sub>2</sub>	8	52	49	44
5% Ba <sub>0.5</sub> KPMo <sub>12</sub> O <sub>40</sub> /ZrO <sub>2</sub>	6	32	33	31

Note: A\* (cm<sup>-1</sup>) is the total area of the absorption bands of nitrate complexes in the 1500–1700 cm<sup>-1</sup> range.

face binding strength for the supported HPCs is lower than for the initial support.

Similar results were obtained for NO<sub>x</sub> adsorption on supported KCu<sub>0.25</sub>PMo<sub>10</sub>SbWO<sub>x</sub>, KCu<sub>0.25</sub>PMo<sub>10</sub>VWO<sub>x</sub>, KCu<sub>0.5</sub>PMo<sub>10</sub>VWO<sub>x</sub>, BaPMo<sub>12</sub>O<sub>x</sub>, and other HPCs (1–5%). By way of example, we present the data obtained for KCu<sub>0.25</sub>PMo<sub>10</sub>VWO<sub>x</sub>/θ-Al<sub>2</sub>O<sub>3</sub> (Fig. 6).

Clearly, the Cu ions in the HPC increase the amount of nitrite and nitrate complexes and increase their binding strength relative to that observed for θ-Al<sub>2</sub>O<sub>3</sub>.

As in the case of θ-Al<sub>2</sub>O<sub>3</sub>, supporting an HPC onto CeO<sub>2</sub> reduces the nitrate complex–surface binding strength. The amount of nitrate complexes on the surface of the CeO<sub>2</sub>-supported samples is much larger than on the support even for NO<sub>x</sub> adsorption at room temperature (Fig. 5). This is likely due to the high activity of the surface oxygen of CeO<sub>2</sub> and the presence of variable-valence ions in the Keggin anion.

It follows from the data listed in Table 3 that supporting 1% KCu<sub>0.25</sub>PMo<sub>10</sub>VWO<sub>x</sub> increases both the amount of nitrate complexes and the strength of their binding to the surface relative to the binnding strength in the case of adsorption on CeO<sub>2</sub>. For the 5% KCu<sub>0.25</sub>PMo<sub>10</sub>VWO<sub>x</sub>/CeO<sub>2</sub> sample, this effect is much weaker. Therefore, variable-valence ions in the Keggin anion reduce the nitrate complex–binding strength, while the ions that are not components of the Keggin anion increase the binding strength. This is true for the CeO<sub>2</sub>- and θ-Al<sub>2</sub>O<sub>3</sub>-based materials and, to a much lesser extent, for the ZrO<sub>2</sub>-based materials. In the latter case, the nitrate complex–surface binding strength is almost invariable. Note that the amount of nitrate complexes on ZrO<sub>2</sub> surface is large even after NO<sub>x</sub> adsorption at room temperature.

## DISCUSSION

This study demonstrated the following:

The unsupported HPCs oxidize NO to NO<sub>2</sub> at room temperature.

Supporting a small amount of an HPC (no more than 1%) increases NO<sub>x</sub> adsorption relative to the adsorption observed for the pure support. This effect is most pronounced for CeO<sub>2</sub> and least pronounced for ZrO<sub>2</sub>.

The main adsorption species are nitrite and nitrate complexes. They are located on the support. As the temperature is raised, the nitrite complexes turn into the nitrate complexes.

Supporting a larger amount of HPC (5%) causes a decrease in NO<sub>x</sub> adsorption relative to the adsorption on the pure support because of the blocking of part of the support surface.

The introduction of vanadium ions into the Keggin anion increases the amount of nitrate complexes and decreases the strength of their binding to the surface relative to what is observed for the pure support. The

**Table 3.** Temperature-dependent amounts of nitrate complexes ( $A^*$ ) for the CeO<sub>2</sub>-based catalysts

Catalyst/ <i>T</i> , °C	30°C	150°C	210°C	280°C
CeO <sub>2</sub>	27	44	44	41
1% KCu <sub>0.25</sub> PMo <sub>10</sub> VWO <sub>x</sub> /CeO <sub>2</sub>	36	101	96	71
5% KCu <sub>0.25</sub> PMo <sub>10</sub> VWO <sub>x</sub> /CeO <sub>2</sub>	55	43	39	20
5% H <sub>n</sub> PMo <sub>11</sub> V <sub>1</sub> O <sub>40</sub> /CeO <sub>2</sub>	62	51	48	36
5% H <sub>n</sub> PMo <sub>9</sub> V <sub>3</sub> O <sub>40</sub> /CeO <sub>2</sub>	62	55	46	35

Note:  $A^*$  (cm<sup>-1</sup>) is the total area of the absorption bands of nitrate complexes in the 1500–1700 cm<sup>-1</sup> range.

substitution of copper ions for protons in the HPC strengthens the nitrate complex–surface binding. The strongest nitrate–surface binding is observed for ZrO<sub>2</sub>, the weakest binding, for θ-Al<sub>2</sub>O<sub>3</sub>.

NO<sub>x</sub> adsorption causes a buildup of hydroxyl groups on the θ-Al<sub>2</sub>O<sub>3</sub> and ZrO<sub>2</sub> surfaces. This effect is not observed for CeO<sub>2</sub>.

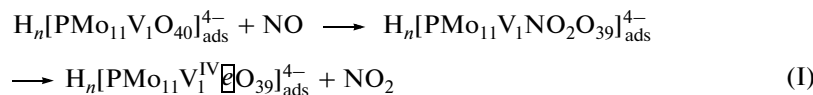
**Table 4.** Effect of the composition of HPC/θ-Al<sub>2</sub>O<sub>3</sub> on the amount of nitrate complexes at different temperatures

Catalyst/ <i>T</i> , °C	30°C	150°C	210°C	280°C
θ-Al <sub>2</sub> O <sub>3</sub>	3	67	73	66
1% H <sub>3</sub> PMo <sub>12</sub> O <sub>40</sub> /θ-Al <sub>2</sub> O <sub>3</sub>	4	68	68	56
1% H <sub>n</sub> PMo <sub>11</sub> V <sub>1</sub> O <sub>40</sub> /θ-Al <sub>2</sub> O <sub>3</sub>	4	69	68	61
1% H <sub>n</sub> PMo <sub>9</sub> V <sub>3</sub> O <sub>40</sub> /θ-Al <sub>2</sub> O <sub>3</sub>	5	71	68	63

Note:  $A^*$  (cm<sup>-1</sup>) is the total area of the absorption bands of nitrate complexes in the 1500–1700 cm<sup>-1</sup> range.

The amount of nitrate complexes on the surface of the HPC-loaded samples is much larger than on CeO<sub>2</sub> even upon NO<sub>x</sub> adsorption at room temperature. This is likely due to the high reactivity of the surface oxygen of CeO<sub>2</sub> and the presence of variable-valence ions in the Keggin anion.

The following scheme of NO interaction with the supported HPA is suggested for explaining the above data:

**Scheme 1.**

The increase in NO adsorption is due to NO oxidation to NO<sub>2</sub> on the HPC surface, and NO<sub>2</sub> forms surface nitrate complexes much more readily than NO.

As follows from the experimental data presented in Fig. 5, NO is more readily oxidizable into NO<sub>2</sub> in the presence of heteropoly salts containing variable-valence ions, such as Cu<sup>2+</sup>. This is apparently due to the fact that the redox properties of the copper ion favor the stabilization of the electrons liberated in step (I).

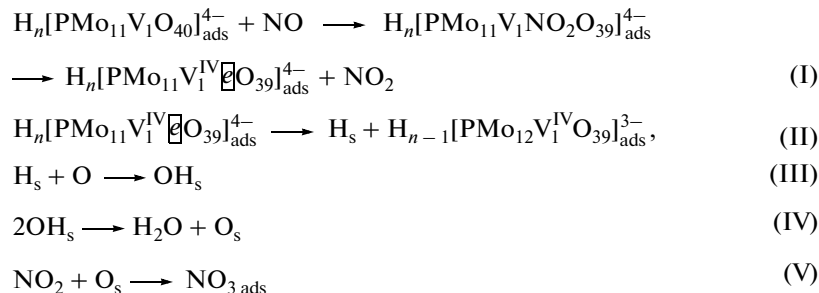
Among the samples examined, ZrO<sub>2</sub> and 1% H<sub>n</sub>PMo<sub>9</sub>V<sub>3</sub>O<sub>40</sub>/CeO<sub>2</sub> contain the largest amounts of nitrate complexes. This fact can likely be explained by

the high activity of the surface oxygen of ZrO<sub>2</sub> for NO adsorption. In this case, intensive NO adsorption takes place without NO preoxidation to NO<sub>2</sub> as well. As a consequence, the decrease in the specific surface area of the support upon the supporting of an HPC at any concentration leads to a decrease in the amount of NO adsorbed.

The hydroxyl groups in the HPA show themselves as broad absorption bands (Fig. 3); it is possible that they are responsible for the broad peak at 2400 cm<sup>-1</sup>. As the HPA content is increased, the absorption intensity in this region remains approximately invariable

and the intensity of the absorption band at  $3370\text{ cm}^{-1}$  increases. To explain the fact that  $\text{NO}_x$  adsorption causes

a buildup of hydroxyl groups on the support surface (Figs. 3, 4), we suggest the following reaction scheme:



Scheme 2.

The oxidation of NO to  $\text{NO}_2$  can be accompanied by a decrease in the charge of the Keggin anion (step (II) in Scheme 2) and, accordingly, by a decrease in the number of protons bound to this anion [38]. The liberated protons form an additional amount of hydroxyl groups (step (III) in Scheme 2). It is due to this circumstance that  $\text{NO}_x$  adsorption increases the number of hydrogen-bonded hydroxyl groups on the  $\theta\text{-Al}_2\text{O}_3$ - and  $\text{ZrO}_2$ -supported heteropoly acid (Figs. 2, 3, 5, 6). By contrast, IR spectra do not indicate the appearance of extra hydroxyl groups on  $\text{CeO}_2$ . According to Qi et al. [37], the surface oxygen of  $\text{CeO}_2$  is extraordinarily mobile. Even vacuum treatment generates vacancies in this material. Owing to the high reactivity of the surface oxygen, the resulting hydroxyl groups recombine rapidly to yield water (step (IV) in Scheme 2).

This mechanism of the interaction of NO with the sample is likely due to the destruction of the supported HPA. This destruction of part of the supported HPC is indirectly indicated by the change in the binding strength of the nitrate complexes located on the support surface in the presence of a small amount (1%) of the active component. The decomposed HPC modi-

fies the support, changing the properties of surface oxygen and, accordingly, the nitrate complex—support binding strength. Further evidence in favor of this support surface modification taking place is that the absorption bands of the nitrate complexes on the HPC-loaded samples are shifted by  $1\text{--}2\text{ cm}^{-1}$  relative to those of the same complexes on the pure support.

It is interesting that the supporting of an HPA or HPC causes a considerable buildup of hydrogen-bonded hydroxyl groups on the support (Figs. 3, 4,  $3000\text{--}3700\text{ cm}^{-1}$ ).

According to NMR and IR spectroscopy data [39–43] and conductivity measurements, the HPA  $\text{H}_3\text{PMo}_{12}\text{O}_{40}$  has two types of protons. One is delocalized, hydrated, highly mobile proton. The other is not hydrated and is less mobile. This type of proton is directly bonded to the Keggin anion.

After supporting the HPA on the support, the hydrated protons localize on the support surface. Upon heat treatment (dehydration), the protons can form hydroxyl bonds with surface oxygen. It is also possible that protons are captured by cationic vacancies on the surface [44, 45]. As a result, supporting the HPC yields rather large amounts of various kinds of hydroxyl groups.

The study of NO adsorption on the supported HPCs demonstrated that, by varying the HPC amount and composition, it is possible to control the amount of adsorbed molecules and the adsorbate—surface binding strength. The amount of adsorbed molecules correlates with the efficiency of NO oxidation to  $\text{NO}_2$ ; the binding strength, with the modification of the support surface via the destruction of part of the supported HPC.

#### ACKNOWLEDGMENTS

This study was supported in part by the Russian Foundation for Basic Research, project no. 08-03-92222-GFEN.

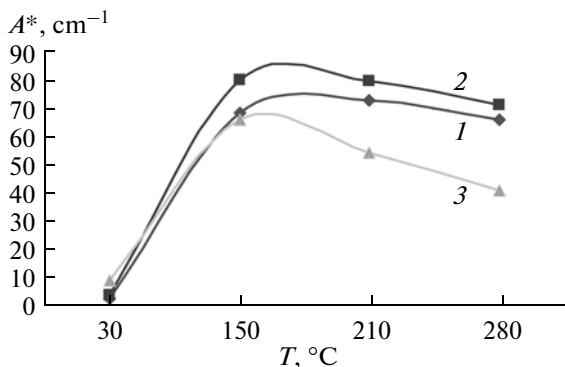


Fig. 6. Temperature dependence of the amount of nitrate complexes (total area of the absorption bands  $v_3$  of the nitrates) for (1)  $\theta\text{-Al}_2\text{O}_3$ , (2) 1%  $\text{KCu}_{0.25}\text{PMo}_{10}\text{VWO}_x/\theta\text{-Al}_2\text{O}_3$ , and (3) 5%  $\text{KCu}_{0.25}\text{PMo}_{10}\text{VWO}_x/\theta\text{-Al}_2\text{O}_3$ .

## REFERENCES

1. Sadykov, V.A., Lunin, V.V., Rozovskii, A.Ya., Matyshak, V.A., and Ross, J., in *Green Chemistry in Russia*, Lunin, V., Tundo, P., and Lokteva, E., Eds., Green Chemistry Series, no. 12, Vénice, Italy: INCA, 2005, p. 45.
2. Matyshak, V.A., Sadykov, V.A., Chernyshov, K.A., and Ross, J., *Catal. Today*, 2009, vol. 145, nos. 1–2, p. 152.
3. Li, M., Yeom, Y.H., Weitz, E., and Sachtler, W.M.H., *J. Catal.*, 2005, vol. 235, p. 201.
4. Gorce, O., Baudin, F., Thomas, C., Da Costa, P., Djéga-Mariadassou, G., *Appl. Catal., B*, 2004, vol. 54, no. 2, p. 69.
5. Maunula, T., Ahola, J., and Hamada, H., *Appl. Catal., B*, 2000, vol. 26, p. 173.
6. Yeom, Y.H., Li, M., Sachtler, W.M.H., and Weitz, E., *J. Catal.*, 2007, vol. 246, p. 413.
7. Eur. Patent 0573672 A1, 1993.
8. Myioshi, N., Matsumoto, S., Katoh, K., Tanaka, T., Harada, K., Takahashi, N., Yokota, K., Sugiura, M., and Kasahara, K., *SAE Tech. Papers*, 1995, no. 950809.
9. Takahashi, N., Shinjoh, H., Iijima, T., Suzuki, T., Yamazaki, K., Yokota, K., Suzuki, H., Myioshi, N., Matsumoto, S., Tanizawa, T., Tanaka, T., Tateishi, S., and Kasahara, K., *Catal. Today*, 1996, vol. 27, p. 63.
10. Lesage, T., Saussey, J., Malo, S., Hervieu, M., Hedouin, C., Blanchard, G., and Daturi, M., *Appl. Catal., B*, 2007, vol. 72, p. 166.
11. Yong Liu, Ming Meng, Zhi-qiang Zou, Xin-gang Li, and Yu-qing Zha, *Catal. Commun.*, 2008, vol. 10, p. 173.
12. Ken-ichi Shimizu, Yoshinori Saito, Takeshi Nobukawa, Naoto Miyoshi, and Atsushi Satsuma, *Catal. Today*, 2008, vol. 139, p. 24.
13. Morandi, S., Prinetto, F., Ghiott, G., Livi, M., and Vaccari, A., *Microporous Mesoporous Mater.*, 2008, vol. 107, p. 31.
14. Fridell, E., Skoglundh, M., Johansson, S., Westerberg, B., Törnerona, A., and Smedler, G., *Stud. Surf. Sci. Catal.*, 1998, vol. 116, p. 537.
15. Fridell, E., Skoglundh, M., Westerberg, B., Johansson, S., and Smedler, G., *J. Catal.*, 1999, vol. 183, p. 196.
16. Coronado, M.J. and Anderson, J.A., *J. Mol. Catal. A: Chem.*, 1999, vol. 138, p. 83.
17. Mahzoul, H., Brilhac, J.F., and Gilot, P., *Appl. Catal., B*, 1999, vol. 47, p. 20.
18. Balcon, S., Potvin, C., Salin, L., Tempere, J.F., and Djéga-Mariadassou, G., *Catal. Lett.*, 1999, vol. 60, p. 39.
19. Fridell, E., Persson, H., Westerberg, B., Olsson, L., and Skoglundh, M., *Catal. Lett.*, 2000, vol. 66, p. 71.
20. Piacentini, M., Maciejewski, M., Bürgi, T., and Baiker, A., *Top. Catal.*, 2004, vols. 30–31, p. 71.
21. Nova, I., Castoldi, L., Prinetto, F., Dal Santo V., Lietti, L., Tronconi, E., Forzatti, P., Ghiotti, G., Psaro, R., and Recchia, S., *Top. Catal.*, 2004, vols. 30–31, p. 181.
22. Nova, I., Lietti, L., and Forzatti, P., *Catal. Today*, 2008, vol. 136, p. 128.
23. Lindholm, A., Currier, N.W., Fridell, E., Yezerski, A., and Olsson, L., *Appl. Catal., B*, 2007, vol. 75, p. 78.
24. Yu Su, Kabin, K.S., Harold, M.P., and Amiridis, M.D., *Appl. Catal., B*, 2007, vol. 71, p. 207.
25. Abdulhamid, H., Fridell, E., Dawody, J., and Skoglundh, M., *J. Catal.*, 2006, vol. 241, p. 200.
26. Frola, F., Prinetto, F., Ghiotti, G., Castoldi, L., Nova, I., Lietti, L., and Forzatti, P., *Catal. Today*, 2007, vol. 126, p. 81.
27. Tikhov, S.F., Sadykov, V.A., Kryukova, G.N., and Paukshtis, E.A., *J. Catal.*, 1992, vol. 134, p. 506.
28. Kuznetsova, T.G. and Sadykov, V.A., *Kinet. Katal.*, 2008, vol. 49, no. 6, p. 886 [*Kinet. Catal.* (Engl. Transl.), vol. 49, no. 6, p. 840].
29. Bethke, K.A., Alt, D., and Kung, M., *Catal. Lett.*, 1994, vol. 25, no. 1, p. 37.
30. Staroverova, I.N., Kutyrev, M.Yu., and Khvitsiashvili, L.G., *Kinet. Katal.*, 1986, vol. 27, no. 3, p. 691.
31. Matyshak, V.A. and Krylov, O.V., *Catal. Today*, 1995, vol. 25, p. 1.
32. Davydov, A.A., *Infrared Spectroscopy of Adsorbed Species on the Surface of Transition Metal Oxides*, New York: Wiley, 1990.
33. Martinez-Arias, A., Soria, J., Conesa, J.C., Seoane, X.L., Arcoya, A., and Cataluna, R., *J. Chem. Soc. Faraday Trans.*, 1995, vol. 91, no. 11, p. 1679.
34. Philopp, S., Drochner, A., Kunert, J., Vogel, H., Theis, J., and Lox, E.S., *Top. Catal.*, 2004, vols. 30–31, p. 235.
35. Daturi, M., Bion, N., Saussey, J., Lavalle, J.-C., Hedouin, C., Seguelong, T., and Blanchard, G., *Phys. Chem. Chem. Phys.*, 2000, vol. 3, p. 252.
36. Soria, J., Martinez-Arias, A., and Conesa, J.C., *J. Chem. Soc. Faraday Trans.*, 1995, vol. 91, no. 11, p. 1669.
37. Qi, G., Yang, R.T., and Chang, R., *Appl. Catal., B*, 2004, vol. 51, p. 93.
38. Servicka, E.M., Bruckman, K., Haber, J., Paukshtis, E.A., and Yurchenko, E.N., *Appl. Catal.*, 1991, vol. 73, p. 153.
39. Chuvayev, V.F., Popov, K.I., and Spitsyn, V.I., *Dokl. Akad. Nauk SSSR*, 1978, vol. 243, p. 973.
40. Kazanski, L.P., Potapova, I.V., and Spitsyn, V.I., *Proc. 3rd Int. Conf. on the Chemistry and Uses of Molybdenum*, Ann Arbor, Mich., 1979, p. 67.
41. Chuvayev, V.F., Popov, K.I., and Spitsyn, V.I., *Dokl. Akad. Nauk SSSR*, 1980, vol. 255, p. 892.
42. Mizumo, M., Katamura, K., Yoneda, Y., and Nisono, M., *J. Catal.*, 1983, vol. 83, p. 384.
43. Nakamura, O. and Ogina, I., *Mater. Res. Bull.*, 1982, vol. 17, p. 231.
44. Dowden, D.A., *J. Chem. Soc.*, 1950, nos. 1–2, p. 242.
45. Tsyganenko, A.A., Smirnov, K.S., Rzhevskiy, A.M., and Mardilovich, P.P., *Mater. Chem. Phys.*, 1990, vol. 26, no. 1, p. 35.